Journal of Membrane Science 550 (2018) 198–207

Contents lists available at ScienceDirect

Journal of Membrane Science

journal homepage: www.elsevier.com/locate/memsci

High performance mixed matrix membranes (MMMs) composed of ZIF-94 filler and 6FDA-DAM polymer

Miren Etxeberria-Benavides[a,f,*], Oana David[a], Timothy Johnson[b], Magdalena M. Łozińska[c], Angelica Orsi[c], Paul A. Wright[c], Stefan Mastel[d], Rainer Hillenbrand[d,e], Freek Kapteijn[f], Jorge Gascon[f]

[a] Tecnalia Research and Innovation, Energy and Environmental Division, 20009 Donostia-San Sebastian, Spain
[b] Johnson Matthey Technology Centre, Blount's Court, Sonning Common RG4 9NH, United Kingdom
[c] EaStCHEM School of Chemistry, University of St Andrews, Purdie Building, North Haugh, St Andrews, Fife KY16 9ST, United Kingdom
[d] CIC nanoGUNE, 20018 Donostia-San Sebastián, Spain
[e] IKERBASQUE, Basque Foundation for Science, 48013 Bilbao, Spain
[f] Catalysis Engineering, Chemical Engineering Department, Delft University of Technology, Van der Maasweg, 2629 HZ Delft, The Netherlands

ARTICLE INFO

Keywords:
Metal organic frameworks
ZIF-94
Mixed matrix membrane
CO_2 capture

ABSTRACT

Carbon capture and storage (CCS) using membranes for the separation of CO_2 holds great promise for the reduction of atmospheric CO_2 emissions from fuel combustion and industrial processes. Among the different process outlines, post-combustion CO_2 capture could be easily implemented in existing power plants. However, for this technology to become viable, new membrane materials have to be developed. In this article we present the development of high performance mixed matrix membranes (MMMs) composed of ZIF-94 filler and 6FDA-DAM polymer matrix. The CO_2/N_2 separation performance was evaluated by mixed gas tests ($15CO_2$:$85N_2$) at 25 °C and 1–4 bar transmembrane pressure difference. The CO_2 membrane permeability was increased by the addition of the ZIF-94 particles, maintaining a constant CO_2/N_2 selectivity of ~22. The largest increase in CO_2 permeability of ~ 200% was observed for 40 wt% ZIF-94 loading, reaching the highest permeability (2310 Barrer) at similar selectivity among 6FDA-DAM MMMs reported in literature. For the first time, the ZIF-94 metal organic framework crystals with particle size smaller than 500 nm were synthesized using nonhazardous solvent (tetrahydrofuran and methanol) instead of dimethylformamide (DMF) in a scalable process. Membranes were characterized by three non-invasive image techniques, i.e. SEM, AFM and nanoscale infrared imaging by scattering-type scanning near-field optical microscopy (s-SNOM). The combination of these techniques demonstrates a very good dispersion and interaction of the filler in the polymer layer, even at very high loadings.

1. Introduction

Carbon dioxide concentration in the atmosphere has been increasing significantly over the past century. Fuel combustion for electricity and heat generation represented by far the largest source in 2014, more than 40% of global CO_2 emissions [1]. These overwhelming contribution suggests that, in addition to the development of energy generation processes that rely on renewable resources, carbon capture and storage (CCS) should be implemented in currently running energy generation plants [2,3]. Three major ways have been considered to reduce CO_2 emissions in combustion processes: pre-combustion CO_2 capture (after coal gasification), post-combustion CO_2 capture from power plant flue gas, and oxyfuel combustion [4].

Since the serial production of commercial polymeric membranes was implemented in 1980 by Henis and Tripodi, membrane gas separation has rapidly become a competitive separation technology. Membrane gas separation offers several benefits over conventional gas separation technologies [5]: lower energy cost, a relatively small footprint, low mechanical complexity and operation under continuous, steady-state conditions.

To date only polymeric membranes have been implemented for gas separation on a large scale in industry, mainly due to their easy processing and mechanical strength [6]. However their performance is limited by the trade-off relationship between permeability and selectivity, represented by the 'Robeson upper bound' [7,8]. Low chemical and thermal stability and plasticization at high pressures in the presence of strong adsorbing penetrants such as CO_2 are among the main disadvantages of this type of membranes. On the other hand, although

* Corresponding author at: Tecnalia Research and Innovation, Energy and Environmental Division, 20009 Donostia-San Sebastian, Spain.
E-mail address: miren.etxeberria@tecnalia.com (M. Etxeberria-Benavides).

https://doi.org/10.1016/j.memsci.2017.12.033
Received 1 August 2017; Received in revised form 6 December 2017; Accepted 13 December 2017
Available online 16 December 2017

Table 1
Literature review: Gas separation performance of 6FDA-DAM based dense MMMs. reported in literature. Pure polymer and mixed matrix membrane separation performance is reported at the same column separated by an arrow (pure polymer → MMM).

Filler	Filler loading (wt%)	CO_2 Permeability (Barrer)	Selectivity			Test	Ref.
			CO_2/N_2	CO_2/CH_4	Propylene/propane		
ZIF − 94	40	770 → 2310	24 → 22	–	–	MG[a]	This work
NH_2-MIL − 53(Al)	20	360 → 660	–	31 → 28	–	MG[b]	[34]
ZIF − 11	20	20.6 → 257	–	33 → 31	–	SG	[35]
Mg-MMS	8	653 → 1214	19 → 24	–	–	MG	[62]
CPO − 27(Mg)	10	650 → 850	14 → 23	–	–	SG	[36]
ZIF − 90	15	390 → 720	–	24 → 37	–	MG	[37]
ZIF − 8	48	Propylene 16 → 56	–	–	12 → 31	MG	[38]

[a] MG corresponds to mixed gas experiment.
[b] SG to single gas experiment.

inorganic membranes based on ceramics [9], carbon [10], zeolite [11], oxides [12], metal organic frameworks (MOF) [13] or metals [14] present an excellent thermal and chemical stability, good erosion resistance and high gas flux and selectivity for gas separation, their implementation at industrial scale has been hampered due to the low mechanical resistance, modest reproducibility, scale-up problems and the high fabrication cost of this type of membranes [13,15].

Mixed matrix membranes (MMMs) were presented as an alternative to overcome limitation of both polymeric and inorganic membranes. In a MMM, filler particles are dispersed in a polymer matrix that should improve the properties of the composite relative to the pure polymer [6,16]. Recently metal organic frameworks (MOFs) have been identified as promising filler materials for the preparation of MMMs [17]. They have high surface area and pore volume and their porosity is in general higher than that of their earlier considered inorganic counterpart, zeolites. Moreover, in contrast with zeolites, due to their partially organic nature, MOFs usually display better polymer-filler compatibility. This prevents formation of non-selective voids at the polymer-filler interface and consequently defect free membranes can be made [18]. One of the first reports of a MOF used in a MMM concerned the additions of copper biphenyl dicarboxylate-triethylene diamine to poly (3-acetoxyethylthiophene (PAET) [19]. Since then quite a few MOF/polymer pairs have been studied in literature [20,21]. Zeolitic imidazolate frameworks (ZIFs) are a subclass of MOFs whit a similar structure of zeolites. Several ZIF/polymer pairs have been studied in literature as MMMs for CO_2/N_2 separation. ZIF-8 was used to improve the permeability of 6FDA–DAM: DABA(4:1) films by Lively et al. [22]. At 20 wt% loading, the membrane permeability increased by 2.5 times over the neat polymer membrane, with only a modest 9.4% loss in CO_2/N_2 selectivity. ZIF-8 was also used as filler by Nafisi et al. [23] and Wijenayake et al. [24] for the preparation of 6FDA-durene MMMs. In both cases an increase on CO_2 permeability was observed due to polymer chain interruption and increase in fractional free volume caused by the filler, 1.5 times higher CO_2 permeability for 30 wt% ZIF-8 loaded membrane and 3.3 times higher for 33.3 wt% loaded respectively. However a slight decrease in CO_2/N_2 selectivity was observed in both cases, attributed to the relatively higher increase in permeability for N_2. ZIF-71 nanoparticles were incorporated to the same polymer by Japip et al. [25]. With a 20 wt% ZIF-71 addition, the pure CO_2 permeability of the MMM was increased by 3-fold, while the ideal CO_2/N_2 selectivity was reduced from 14.7 to 12.9.

Different ZIF fillers have been added to Pebax polymer matrix. ZIF-8 filler and Pebax 2533 polymer matrix was used by Nafisi et al. [26] to prepare self-supported dual layer mixed matrix membranes. CO_2 permeability was increased by 3.6 times by the addition of 35 wt% ZIF-8, while a slight decrease on CO_2/N_2 selectivity was observed. In other study, an asymmetric membrane was prepared by Li et al. [27] by depositing a thin mixed matrix layer of < 1 mm of Pebax 1657 and ZIF-7 on a porous polyacrylonitrile support. An intermediate gutter layer of PTMSP was applied to serve as a flat and smooth surface for coating to avoid polymer penetration into the porous support. CO_2 permeability was increased by 1.5 times and CO_2/N_2 selectivity was tripled by the addition of 22 wt% ZIF-7 filler. The enhanced performance was attributed to the combination of molecular sieving effect from ZIF-7 filler and the high solubility of CO_2 in Pebax.

In the present work ZIF-94 particles have been prepared and incorporated into 6FDA-DAM to form MMMs with the aim of achieving membrane properties similar to those recommended by Merkel *et al.* for the post-combustion CO_2 capture (the focus of this paper). 6FDA-based polyimides possess impressive gas separation performance, pairing high permeability with good permselectivity. Their rigid primary structure contains bulky CF_3 groups through which the efficient packing of polymeric chains is inhibited and local segment mobility is reduced [28]. Many other desirable properties such as spinnability, thermal and chemical stability and mechanical strength as compared with non-fluoropolyimides make this polymer family suitable for gas separation applications [29–33]. In our case, a commercially available high flux 6FDA-DAM polyimide was selected for membrane preparation. The preparation of 6FDA-DAM MMMs by the addition of several fillers such us NH_2-MIL-53(Al) [34], ZIF-11 [35], CPO-27(Mg) [36], ZIF-90 [37] and ZIF-8 [38] has been reported in literature. Membrane properties for gas separation are shown and compared with our MMM in the results and discussion section of this paper (Table 1). The selection of MOF filler was first based on CO_2 adsorption capacity and selectivity over N_2. ZIF-94 (also known as SIM-1, Substituted Imidazolate Material-1) has the **sod** topology and it is constructed by Zn atoms and 4-methyl-5 imidazole-carboxaldehyde (aImeIm) linkers. It has a high CO_2 uptake of 2.4 mmol g^{-1} at 1 bar, higher than its topological counterpart ZIF-93 with the **rho** topology (1.7 mmol g^{-1}, 17.9 Å pore diameter) or other MOFs such as ZIF-7 (1.6 mmol g^{-1}, 7.5 Å pore diameter) and ZIF-11 (0.8 mmol g^{-1}, 14.9 Å pore diameter). The higher CO_2 uptake is attributed to the smaller pore diameter of ZIF-94 (9.1 Å) compare to other ZIFs. As it was reported, small pores are advantageous when considering CO_2 adsorption in the low-pressure regime [39]. ZIF-94/SIM-1 has already been used as membrane material in some publications. Marti *et al.* [40] reported the fabrication of SIM-1 membranes by post synthetic modification of ZIF 8 particles for the separation of water from water/ethanol mixtures. The membrane fabricated using nano SIM-1 crystals separated water completely from the mixture. SIM-1 membrane for CO_2/N_2 separation has been crystallized in situ on a tubular asymmetric alumina support by Aguado *et al.* [41]. In a recent study, layered ZIF/polymer hollow fiber membranes for H_2/CH_4 and CO_2/CH_4 separation were prepared by Cacho-Bailo *et al.* growing a continuous ZIF-94 layer on the bore side of a porous P84 polyimide hollow fiber [42].

ZIF-94 also meets several highly important requirements for product development: (i) Preparation as nanoparticles for inclusion in thin membranes (< 1 μm as target), (ii) scale up production via green

synthesis, using non- or less toxic solvents such as water, THF or DMSO, (iii) low cost of metals and linkers and (iv) stability in water vapor. Prior to up scaling, the synthesis of the ZIF-94 MOF was optimized at the lab scale to yield particles in accordance with membrane fillers requirements.

Here we report the preparation, characterization and performance of unique mixed matrix membranes made of highly engineered materials ZIF-94 and 6FDA-DAM. The membranes have remarkable gas separation properties tested under process conditions relevant for CO_2 capture in post-combustion applications.

2. Experimental section

2.1. Materials

6FDA-DAM (Mn = 170,177 Da, T_g = 395 °C) was purchased from Akron Polymer Systems (USA). ZIF-94 particles were synthesized solvothermally. For lab scale synthesis zinc acetate dehydrate was purchased from Sigma-Aldrich and 4-methyl-5-imidazolecarboxaldehyde from Maybridge. For up scaling, zinc acetate dihydrate and 4-methyl-5-imidazolecarboxaldehyde were purchased from Acros Chemicals (98% and 99% purity respectively). Methanol (99.8%) and anhydrous tetrahydrofuran (≥99.9%) were supplied by Sigma-Aldrich.

2.2. Synthesis of ZIF-94 crystals

The synthesis of the ZIF-94 particles was first optimized at the lab scale and then scale up. Lab scale synthesis of ZIF-94 involved dissolving 0.4392 g of $Zn(CH_3COO)_2{\cdot}2H_2O$ (2 mmol) in 20 mL of methanol and 0.4404 g of 4-methyl-5-imidazolecarboxaldehyde (aImeIm, 4 mmol) in 50 mL of THF. For up scaling, 3.52 g of $Zn(CH_3COO)_2{\cdot}2H_2O$ (160 mmol) were dissolved in 160 mL of methanol and 3.52 g of 4-methyl-5-imidazolecarboxaldehyde (aImeIm, 31 mmol) in 400 mL of THF. After the solids were completely dissolved, $Zn(CH_3COO)_2{\cdot}2H_2O$-methanol solution was poured slowly into the aImeIm-THF solution. The mixture was continuously stirred for 60 mins at room temperature (30 mins for up scaling). The product was collected by centrifugation and washed with methanol three times before drying at room temperature (at 105 °C for up scaling).

2.3. ZIF-94 characterization

Scanning electron micrographs were obtained from a JEOL JSM-6700F FE-SEM. Samples were sputter coated three times with gold in a Quorum Q150R ES (10 mA, 30 s and 2.3 tooling factor).

Powder X-ray diffraction (PXRD) data of lab scale sample was collected in Debye-Scherrer (capillary) geometry from STOE STAD i/p diffractometers with primary monochromation (Cu $K_{\alpha1}$, λ = 1.54056 Å). Prior to analysis, samples were ground to a fine powder and introduced to a 0.7 mm glass capillary. PXRD pattern of up scaled sample was collected using a Bruker AXS D8 diffractometer using Cu Kα radiation (λ = 1.5406 and 1.54439 Å) over the 2θ range of 3–130° in 0.02° steps. Powder was places on a PTFE sample holder and analyzed in Bragg-Brentano reflection geometry. Le Bail refinement was performed using Topas with reflection profiles modelled using a fundamental parameters approach [43] with reference data collected from NIST660 LaB_6.

N_2 (−196 °C) adsorption isotherms were measured on a Micromeritics 2020 volumetric instrument (lab scale sample) and Quantachrome Autosorb iQ instrument (up scaled sample). CO_2 (25 °C, 1 bar) adsorption isotherm was measured on a Hiden IGA porosimeter. Lab scale sample was activated at 120 °C for 6 h under vacuum and up scaled sample at 200 °C for 12 h prior to adsorption measurements.

Thermogravimetric analysis (TGA) data was acquired for lab scale samples (~ 3 mg) in the temperature range 15 − 800 °C at a heating rate of 5 °C min^{-1} in flowing air. Up-scaled sample was collected on a Netzsch TGA 760 between room temperature and 1000 °C heating at 3 °C min^{-1} in 80:20 Ar:O_2.

2.4. Membrane preparation

6FDA-DAM/ZIF-94 MMMs were prepared at different MOF loadings (10, 20, 30 and 40 wt%). Up-scaled ZIF-94 was used for membrane preparation. For comparison purposes, the pure polymer membrane was also prepared. Membranes were prepared by a casting method. Polymer and MOF were dried in a vacuum oven at 100 °C overnight before casting solution preparation. A polymeric pre-dope composed of 13 wt% 6FDA-DAM in THF was prepared. ZIF-94 was dispersed in tetrahydrofuran in an ultrasonic bath for 1 h. The polymeric pre-dope was added to the ZIF-94/THF suspension and was stirred overnight at room temperature. The solvent/filler-polymer ratio of the final solution was of 91/9. Solution was cast with a dr. Blade over a glass plate (casting thickness of 80 μm) and solvent evaporated at room temperature for 24 h in a solvent rich environment. Membranes were heat treated in a vacuum oven at 160 °C overnight to eliminate residual solvent. Membrane thickness was measured with a digital micrometer (Mitutoyo) at different locations of the membrane. The average thickness value of ten measurements was used for permeability calculations.

2.5. Membrane characterization

The surface and cross-section morphology of the dense MMMs were characterized by scanning electron microscopy (SEM) (Quanta 250 ESEM) equipped with energy dispersive X-ray spectroscopy (EDX). The samples for cross-section SEM characterization were prepared by freeze-fracturing in liquid nitrogen. The low voltage high contrast backscatter electron detector (vCD) and the large field detector (LFD) were used for the analysis of the membranes.

Fourier transform infrared spectroscopy (FTIR) of pure components was performed on a Vertex 70 instrument (Bruker). Infrared chemical mapping of the MMMs with nanoscale spatial resolution was performed with a scattering-type scanning near-field optical microscope (IR s-SNOM) [44] (neaSNOM, Neaspec GmbH, Germany). It is based on an atomic force microscope (AFM), where the tip is illuminated with monochromatic infrared radiation of frequency ω. Recording of the tip-scattered infrared field with a pseutoheterodyne interferometer yields infrared amplitude and phase images simultaneously with topography [45]. Strong phase contrast reveals areas of strong molecular vibrational absorption [46,47]. We used standard Pt-coated AFM tips for both topography and infrared imaging, and a frequency-tunable quantum cascade laser (QCL) (MIRcat, Daylight Solutions Inc., USA) for tip illumination.

Permeation experiments were performed for pure gases and CO_2/N_2 gas mixtures in the gas permeation setup described elsewhere [48]. Circular samples of 3.14 cm^2 were cut and placed in the permeation cell over a macroporous stainless steel SS 316 L support with 20 μm nominal pore size. Gas was fed at 25 °C and different pressures (1–4 bar transmembrane pressure difference). Transmembrane pressure was adjusted using a back-pressure regulator at the retentate side while permeate side of the membrane was kept at atmospheric pressure. A CO_2/N_2 gas mixture (15:85) was used as feed gas for mixed gas experiments (20 mL min^{-1} CO_2 and 113 mL min^{-1} N_2) and helium (3 mL min^{-1}) as sweep gas at the permeate side. An online gas chromatograph (Interscience Compact GC) equipped with a packed Carboxen 1010 PLOT (30 m × 0.32 mm) column and thermal conductivity detector (TCD) and flame ionization detector (FID) was used to analyze permeate stream composition over time. Permeability was calculated once the steady state was reached in the permeate stream of the membrane. Two samples of each membrane were tested and average values of two membranes are reported.

The permeability for gas *i* was calculated by the following equation:

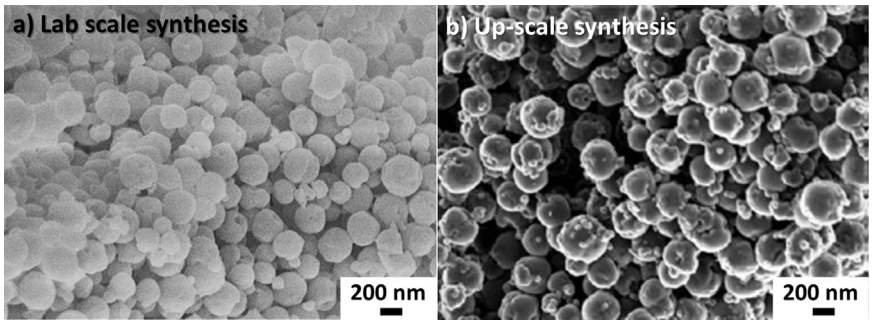

Fig. 1. SEM image of (a) lab scale and (b) up-scale synthesized ZIF-94 particles.

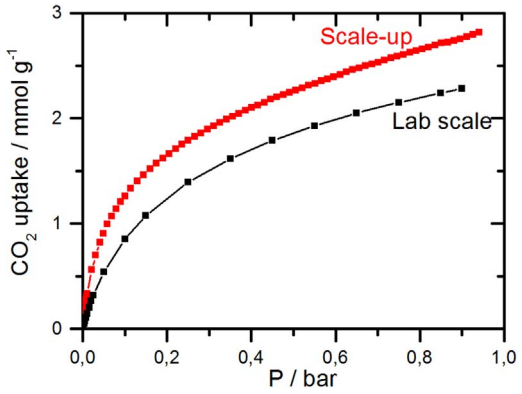

Fig. 2. CO_2 adsorption isotherms of lab scale and up-scale ZIF-94 at 25 °C.

$$P_i = \frac{F_i \cdot l}{\Delta p_i \cdot A}$$

where P_i is the gas permeability in Barrer (1 Barrer = 10^{-10} cm^3 (STP) cm cm^{-2} s^{-1} $cmHg^{-1}$), F_i is the volumetric flow rate of component i (cm^3 (STP)/s), l is the thickness of the membrane (cm), Δp_i is the partial pressure difference of component i across the membrane (cmHg) and A is the effective membrane area (cm^2).

The separation factor or mixed gas selectivity α was calculated as the ratio of the permeability of more permeable compound i to the permeability of the less permeable compound j:

$$\alpha_{i/j} = \frac{P_i}{P_j}$$

3. Results and discussion

3.1. MOF characterization

ZIF-94 crystals were synthesized in this work by replacing dimethylformamide (DMF), previously used for synthesis of ZIF-94 [39], with a 2:5 ratio mixture of methanol: THF. A reaction yield of 82% for lab scale synthesis and 99% for up scaling, with respect to zinc were achieved. Higher reaction yield might be due to the use of a high-speed centrifuge for up-scale synthesis, not available for lab scale synthesis. The SEM image shown in Fig. 1 indicates that spherical particles of ZIF-94 were produced with a diameter of 100–500 nm. The PXRD pattern of this material (Fig. S1, Supporting information) was consistent with that reported by Aguado et al. [49] and with the sodalite topology.

CO_2 adsorption capacities at 25 °C were 0.85 mmol g^{-1} at 0.10 bar and 2.3 mmol g^{-1} at 0.9 bar for lab scale synthesis and 1.25 mmol g^{-1}

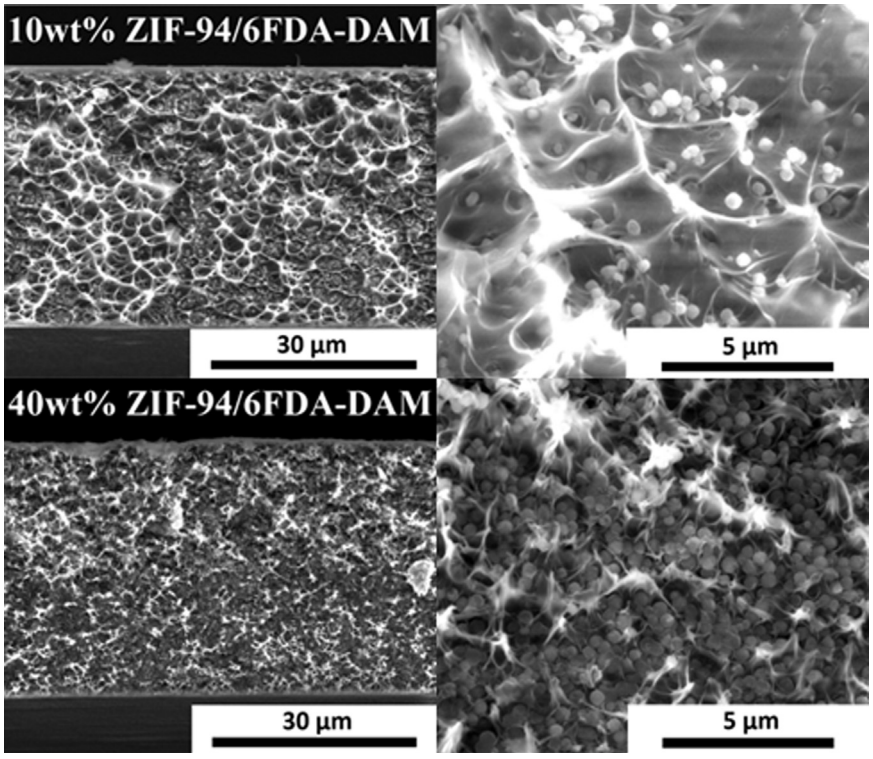

Fig. 3. SEM images of the cross-section of 10 wt% and 40 wt% ZIF-94/6FDA-DAM MMMs obtained by the LFD detector at different magnifications.

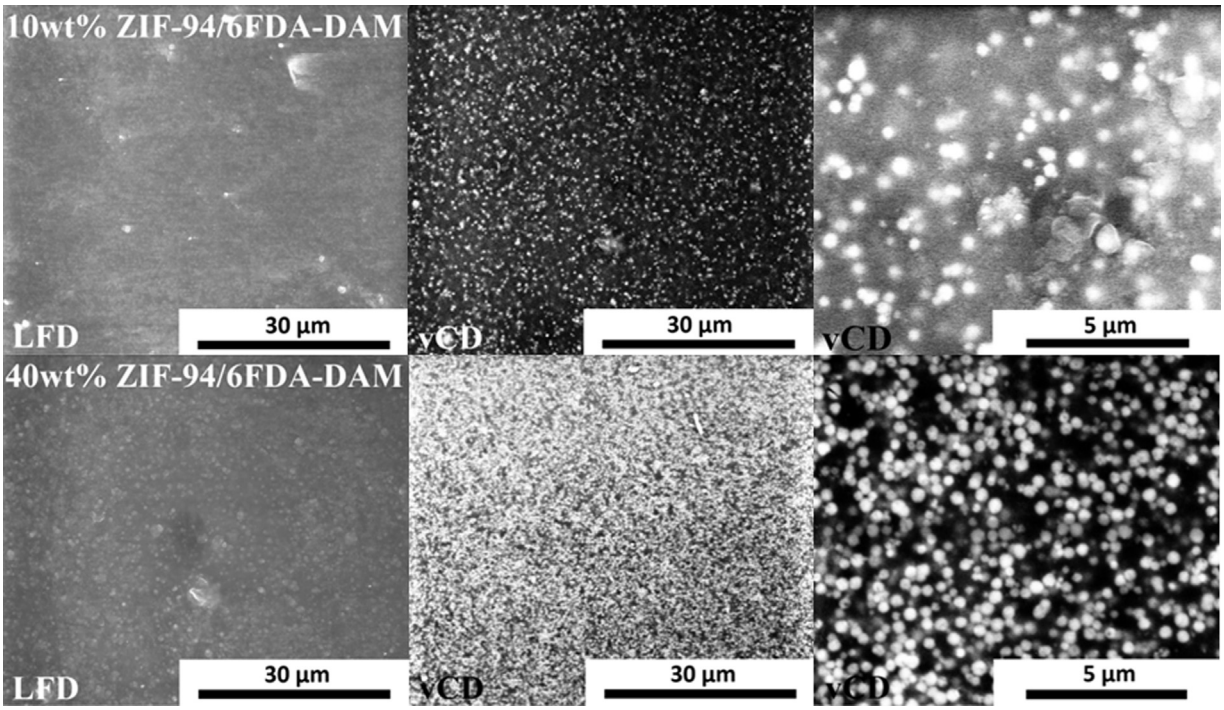

Fig. 4. SEM images of the surface of 10 and 40 wt% ZIF-94/6FDA-DAM MMMs obtained by LFD detector and vCD detector at different magnifications.

at 0.10 bar and 2.75 mmol g^{-1} at 0.9 bar for up scaling (Fig. 2). The BET surface area derived from the N_2 isotherm were 424 m^2 g^{-1} and 506 m^2 g^{-1} respectively (Fig. S2), which is close to what has previously been reported (471 and 480 m^2 g^{-1}) [39,50]. TGA analysis of the as-prepared ZIF-94 in air showed a thermal stability up to ~225 °C with ~20% weight loss due to THF and methanol removal (Fig. S3).

The scale-up of the synthesis from the laboratory small scale to the laboratory pilot scale was achieved for ZIF-94. The characteristics of the resulting up-scaled sample match on the whole those of the solid produced at smaller scale, both in terms of crystallinity, purity and particle size and shape.

3.2. MMMs morphology

6FDA-DAM MMMs were prepared at 10, 20, 30 and 40 wt% ZIF-94 loadings. SEM images of the cross-section of a 10 wt% and 40 wt% ZIF-94 MMM are shown in Fig. 3. A good dispersion of ZIF-94 particles in the polymer matrix was obtained without agglomeration even at high loadings. SEM images of the surface of the ZIF-94 MMMs analyzed using LFD and vCD detectors are shown in Fig. 4. The use of the LFD detector allows analyzing the topography of the surface whereas the compositional contrast provided by the vCD detector allows observing the MOF distribution just beneath the surface of the membrane. The images taken by the LFD detector show a defect free surface, while the presence of MOF particles is visible through the thin transparent polymer surface layer. The presence of the MOF particles under this polymer surface layer is better demonstrated by the vCD detector, since heavier elements such as metal atom of the MOF are brighter in vCD images. For an organic polymer at 20 kV the beam could go up to 5 µm depth into the sample. At the voltage used for SEM analysis (10 kV) it is estimated that the beam might go up to 2 or 3 µm. ZIF-94 particles appear with bright contrast in the vCD image. The good filler distribution might be due to a good compatibility between the polymer phase and ZIF-94 particles expected from interaction of CHO pending group of the MOF linker with -NH_2 end group of the polymer.

XRD patterns of ZIF-94 powder, 6FDA-DAM polymer and MMMs with ZIF-94 loadings of 10–40 wt% are shown in Fig. 5. Pure 6FDA-DAM polymer shows a typical broad spectrum of an amorphous polymer with no crystalline reflections. The diffraction pattern observed for the MMMs confirms the presence of the ZIF-94 phase. ZIF-94 crystalline structure remained unchanged in the MMMs, suggesting that the membrane preparation procedure does not affect the crystallinity of MOF particles.

The infrared characterization of the 40 wt% ZIF-94 MMM is shown in Fig. 6. From FTIR spectroscopy of the pure membrane and pure ZIF-94 reference samples (Fig. 6a), we determined the infrared frequencies for s-SNOM imaging (indicated by dashed lines). At 1665 cm^{-1}, the ZIF-94 exhibits a strong absorption of the -N-H bond vibration, where the polymer absorption is weak. Consequently, the infrared s-SNOM phase image at 1665 cm^{-1} (Fig. 6d) exhibits a strong phase contrast revealing the individual ZIF-94 particles (bright disk-shaped objects), which are collocated with the surface protrusions seen in the AFM

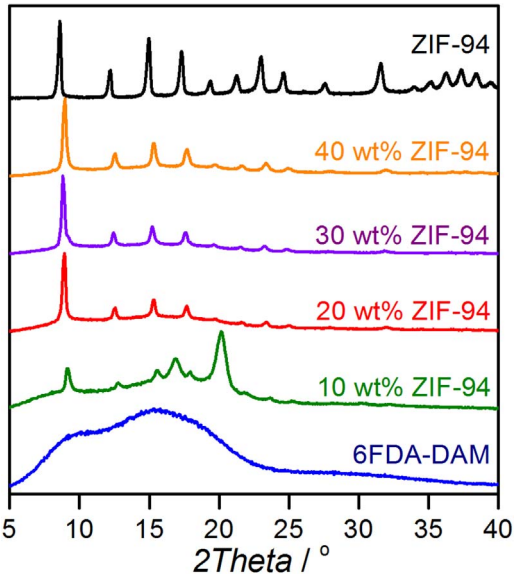

Fig. 5. XRD patterns of ZIF-94 powder, pure 6FDA-DAM membrane and MMMs with different ZIF-94 loadings.

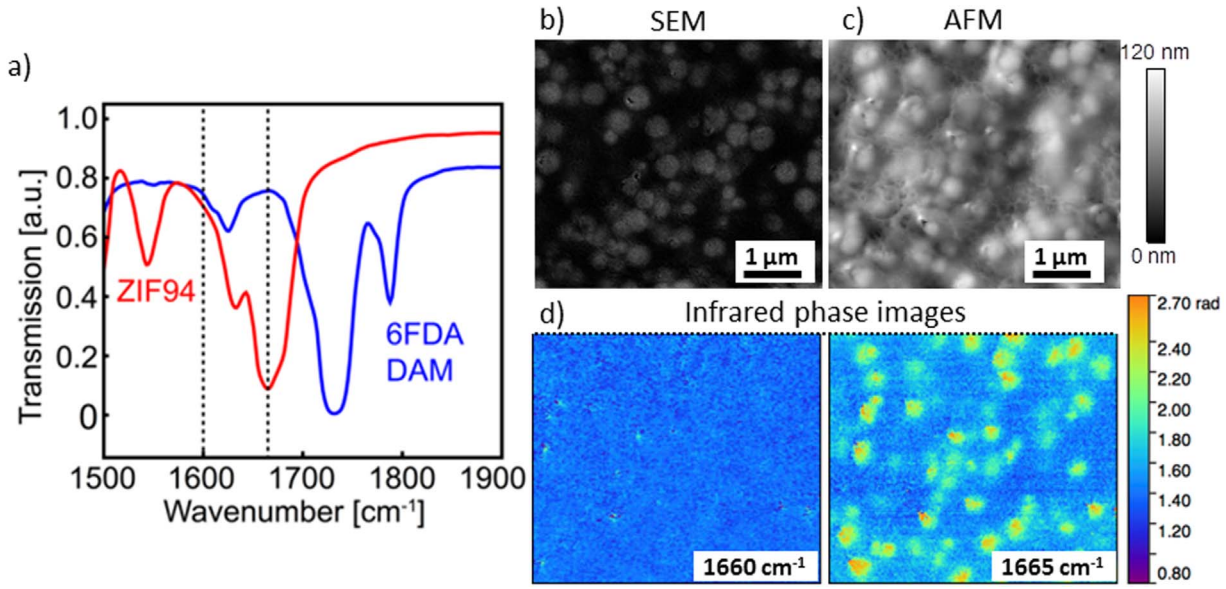

Fig. 6. Infrared characterization of the 40 wt% ZIF-94 MMM surface. (a) Far-field transmission FTIR spectra of pure 6FDA-DAM and ZIF-94, (b) SEM surface image obtained by LFD detector, (c) AFM surface topography and (d) infrared images of the membrane surface.

topography image of exactly the same sample area (Fig. 6c). Furthermore, the contrast of the individual particles strongly varies, which we attribute to their vertical position in the membrane: In s-SNOM, a decreasing contrast of objects of the same size and chemical compositions indicates an increasing depth below the surface [51]. To verify that molecular chemical contrast is observed, another infrared image was recorded at 1600 cm^{-1} (indicated by dashed line in Fig. 6a), where the absorption of both 6FDA-DAM and ZIF-94 is weak. Indeed, the infrared phase image at 1600 cm^{-1} does not show significant contrast. In the future, s-SNOM could be applied for more detailed nanoscale studies, for example of inhomogeneities, and chemical interaction, particularly at the interfaces between individual membrane components [52].

3.3. Gas permeation

3.3.1. Pure polymer: pure gases vs mixed gases for 6FDA-DAM membrane

To date, most of the permeation data reported in literature is for pure gases. In most cases transport behavior of gas mixtures through membranes is different from that of pure gases [52,53]. This leads to differences in pure gas and mixed gas permeabilities and selectivities. Hence, in order to assess membrane properties under real process conditions, it is essential to determine mixed gas permeation performance.

The bare 6FDA-DAM membrane was tested both for pure gases (CO_2 and N_2) and CO_2/N_2 gas mixtures (15:85) at different transmembrane pressure differences (1–4 bar). Single and mixed gas permeabilities (CO_2 and N_2) and CO_2/N_2 selectivities are presented as a function of transmembrane pressure in Fig. 7. For pure CO_2, permeability decreased with increasing feed pressure (from 540 to 450 Barrer at 1 and 4 bar, respectively), a behavior predicted by the dual-mode sorption and mobility models for gas permeation of condensable gases such as carbon dioxide in glassy polymers [54]. Meanwhile the permeability of the low adsorbing penetrant N_2 exhibited little or no dependency on pressure [54]. As a result, a slight decrease in the ideal CO_2/N_2 selectivity was observed with increasing feed pressure for pure gases. It is worth mentioning that another phenomenon that can influence gas permeation through membranes is plasticization, i.e. sorption induced swelling of the polymer matrix, causing an increased polymer chain mobility and consequently increased gas permeability. For 6FDA-DAM polymer, plasticization with CO_2 takes place at pressures higher than 10 bar [55]. Therefore, plasticization is excluded to interfere under the studied conditions.

As expected, significant differences between pure and mixed gas permeation are observed. The mixed gas permeability for N_2 is lower than the pure gas permeability. In the case of CO_2, at first sight the mixed gas permeability seems higher than the pure gas permeability but, if instead of the total feed pressure, one takes into account the partial CO_2 transmembrane pressure difference (from 0.15 to 0.60 bar) then the values for CO_2 permeability fit the trend of higher permeability at lower pressures. The dual-mode sorption model for gas permeation estimates lower permeability for all mixture components due to competitive sorption between gases for the polymer matrix sorption sites. Nevertheless, CO_2 has a much higher affinity constant and solubility in glassy polymers than N_2. Therefore polymer matrix sorption sites are saturated with CO_2, and N_2 permeability is decreased. Similar to pure gases, a decrease in CO_2 permeability was also observed as the transmembrane pressure increased in the mixed gas test (from 768 to 670 Barrer at 1 and 4 bar, respectively). Furthermore, also a small increase in N_2 permeability with increasing pressure was observed, resulting in an unchanged CO_2/N_2 separation factor.

An ideal CO_2/N_2 selectivity of around 14 was obtained based on pure gas permeation, whereas the CO_2/N_2 separation factor for the mixed gas test was 24 over the whole total transmembrane pressure difference range from 1 to 4 bar. This emphasizes the importance of performing mixed gas experiments in order to know membrane performance under relevant conditions for commercial applications. Hence only mixed gas performance is reported below for the MMMs prepared in this work.

3.3.2. MMMs: Effect of ZIF-94 loading on mixed gas separation performance

6FDA-DAM / ZIF-94 MMM were prepared at different MOF loadings (10–40 wt%). Mixed gas separation performance of the bare polymer membrane and MMMs with various loadings of ZIF-94 is shown in Fig. 7. Both CO_2 and N_2 permeability gradually increased when ZIF-94 loading was increased from 0 to 30 wt%, from 770 to 1225 Barrer of CO_2, respectively. A further strong increase in permeability was observed at 40 wt% ZIF-94 loading. CO_2 permeability nearly doubled up to 2310 Barrer at 1 bar transmembrane pressure difference, while the CO_2/N_2 selectivity remained unchanged by the addition of the ZIF-94 at an average value of 22.7 ± 1.5 (results slightly deviate for 30 wt% loading). The increased CO_2 permeability with filler loading might be

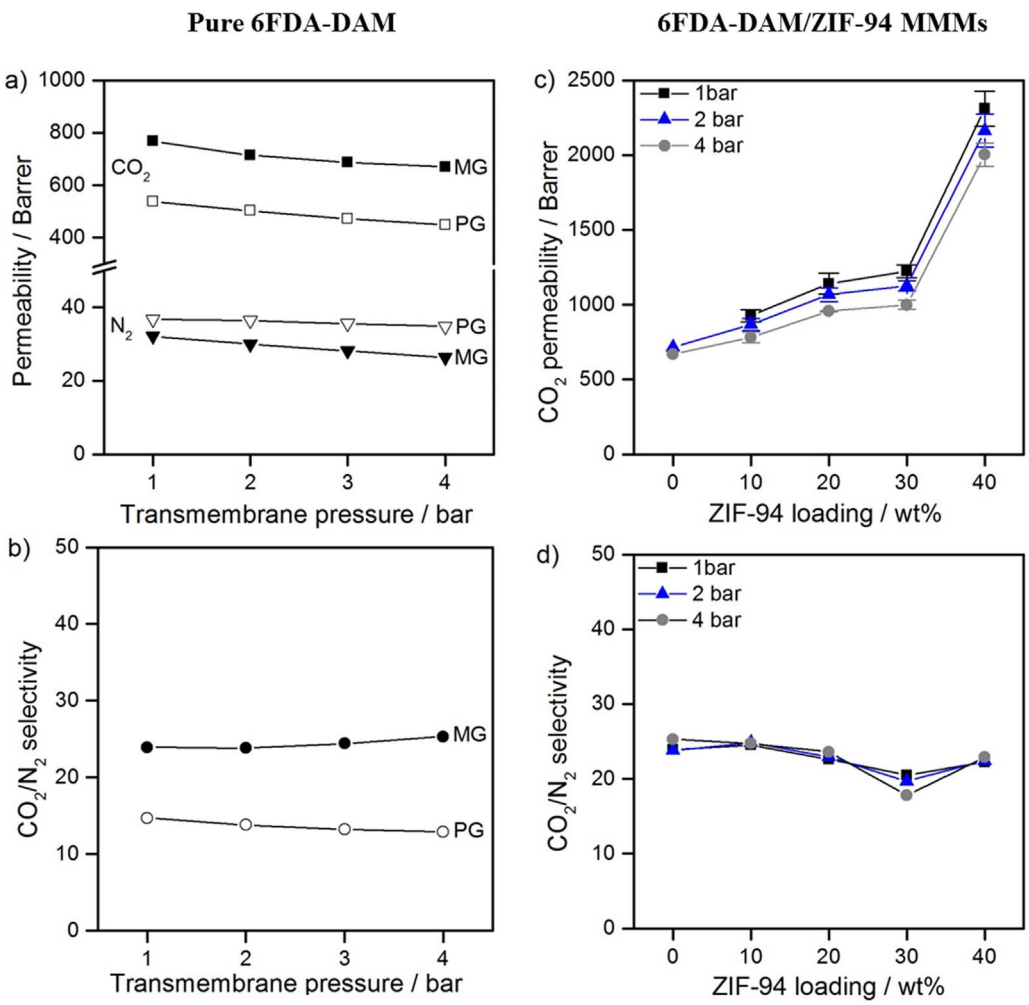

Fig. 7. (a) CO_2 and N_2 permeability and (b) CO_2/N_2 selectivity of 6FDA-DAM membrane for pure gas (PG) and mixed gas (MG) experiments as a function of transmembrane pressure. Experimental results of mixed gas (c) CO_2 permeability and (d) CO_2/N_2 selectivity of prepared MMMs at as a function of ZIF-94 loading and 1–4 bar transmembrane pressure. The data are average values of two samples and error bars correspond to standard deviation. Experiments were performed at 25 °C. The lines are to guide the eye.

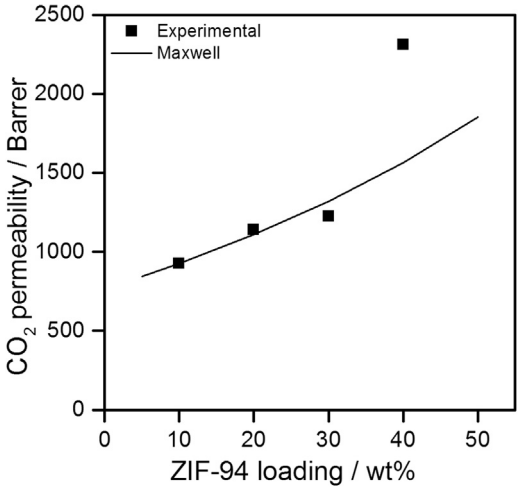

Fig. 8. Experimental mixed gas CO_2 permeability results (square symbols) and permeability predicted by Maxwell equation (line) as a function of ZIF-94 loading at 25 °C and 1 bar trans-membrane pressure.

related to (1) disruption of the chain packing of the polymer, (2) porosity introduced by MOF particles [34] and (3) increase in the polymer free volume [56–58]. The characterization of the MMM shows that in our case the MOF distribution is quite even throughout the membrane with good adhesion between the MOF filler and the polymer. Therefore, the permeability of MMMs is evaluated by the Maxwell equation [6].

First, the unknown parameter of the Maxwell equation P_d (disperse phase permeability) was calculated from experimental 10 wt% membrane permeability, whereas P_c (continuous phase permeability) was determined from the pure polymer permeation. P_d could in principle be determined experimentally from films made of pure MOF. Preparing such films is extremely challenging if not impossible because they should be self-supported with MOF phase densely packed, with no sub-nanometer defects between filler particles. MOF phase with such morphology was achieved only by in situ synthesis on top of porous supports [60] and was not the subject of this study. ZIF-94 (SIM-1) membrane has been crystallized in situ on a tubular asymmetric alumina support with pore size of 200 nm by Aguado *et al.* [41]. They demonstrate that the gas transport obeys the Knudsen diffusion mechanism such as found for microporous membranes. This is translated in higher gas permeability than in polymers and low (Knudsen) gas selectivity. At 35 °C they have achieved overall single gas CO_2 permeance of 104 GPU. Considering the reported MOF layer thickness was of approximately 25 μm and no resistance to the overall transport by the support, we estimate the pure ZIF-94 phase permeability by multiplying permeance with layer thickness to a value of 2613 Barrer. This value is related to pure gas permeation. Our estimated P_d from the 10 wt% experiment represents the mixed gas permeability and was equal to 4735 Barrer.

Then theoretical MMM permeabilities have been predicted for other loadings. The experimental and predicted permeability are presented in Fig. 8. Experimental permeability values of 10–30 wt% loaded membranes follow the trend predicted by the Maxwell relation. However, a higher experimental permeability than predicted is obtained for the 40 wt% loaded membrane. The lack of significant change in selectivity

with MOF loading relative to the bare polymer demonstrates that the prepared MMMs are 'defect-free' and suggests that the polymer determines the selectivity, while the MOF introduces faster transport pathways. The larger permeability than predicted according to the Maxwell model indicates that at high loadings the ZIF-94 influence is not captured by this model, which is approximately only valid up to volume fractions of 20%.

The results obtained in this work follow the general trend reported in a recent review about MOF based MMMs published by Seoane et al. [21]. In most studies, improvements in flux at constant selectivities with respect to the bare polymer have been reported. Only in circa 10% of cases improvements in both flux and selectivity were achieved. In order to benchmark our results with literature, separation performance of 6FDA-DAM based dense MMMs reported in literature are shown in Table 1. In terms of CO_2 permeation through pure polymer we can observe different results. Polymers used in literature were synthesized in the laboratory and different molecular weight could lead to differences in gas separation performance. Also, as 6FDA-DAM has a high free volume, the solvent used for the fabrication of the membrane and the membrane history might influence final separation performance of the membrane. Also, it is worth to mention that we compare single with mix gas results. Nevertheless, the common feature is a significant increase in CO_2 permeability observed by the addition of the filler particles in the 6FDA-DAM polymer matrix. In some cases, there is a selectivity increase due to either molecular sieving [37] or to solubility increase ([36]. Zhang *et al.* went a step further and ZIF-8/6FDA-DAM mixed-matrix hollow fiber membranes were prepared with ZIF-8 nanoparticle loading up to 30 wt% [61]. The mixed-matrix hollow fibers showed significantly enhanced propylene/propane selectivity that was consistent with mixed-matrix dense films.

We extend the benchmarking of our best membrane via a Robeson plot in Fig. 9, including the most relevant results reported in literature for MOF based MMMs for the separation of CO_2 from N_2 [21] for pure gas permeation (•). The separation performance of the 40 wt% ZIF-94 loaded membrane developed in this work (☆) is situated on the Robeson limit and presents the highest permeability at similar selectivity among 6FDA-DAM MMMs reported in literature. Other membranes situated on the Robeson limit are (a) 30 wt% ZIF-8 loaded 6FDA-durene MMM (2185 Barrer CO_2, ideal CO_2/N_2 selectivity 17, point *i* in Fig. 9), (b) 30 wt% Zn_2(1,4-bdc)$_2$dabco loaded 6FDA-4MPD MMM (3300 Barrer CO_2, ideal CO_2/N_2 selectivity 19.1, point *k* in Fig. 9) and (c) 30 wt% loaded PIM-1 membrane (6300 Barrer CO_2, ideal CO_2/N_2 selectivity 18, point *n* in Fig. 9). Their performance has been only tested for pure gases (ideal selectivity) while our membranes have been tested under relevant process conditions (mixed gas 15/85 CO_2/N_2).

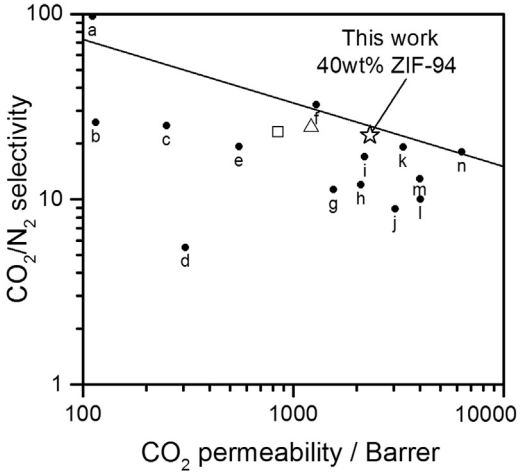

Fig. 9. Robeson plot for the separation of CO_2 from N_2. The graph contains the most relevant results reported in literature for MOF based MMMs (•): (a) Pebax®/ZIF-7 [27], (b) PPO/HKUST-1 [63], (c) XLPEO/CPO-27(Mg) [36], (d) PMDA-ODA/HKUST-1 [64], (e) 6FDA-DAM:DABA 4:1 /ZIF-8 [22], (f) Pebax®/ZIF-8 [26], (g) 6FDA-durene/ZIF-8 [24], (h) PDMS/CPO-27(Mg) [36], (i) 6FDA-durene/ZIF-8 [23], (j) PDMS/HKUST-1 [65], (k) 6FDA-4MPD/[Zn_2(bdc)$_2$(dabco)]·4DMF·0.5H_2O [66], (l) PDMS/[Zn_2(bdc)$_2$(dabco)]·4DMF·0.5H_2O [66], (m) 6FDA-durene/ZIF-71 [25] and (n) PIM-1/ZIF-8 [67]. Separation performance of 6FDA-DAM MMMs reported in literature is represented by △ [59] and □ [36]. Separation performance of ZIF-94/6FDA-DAM MMM prepared in this work is represented by ☆. 1 Barrer = 1 GPU for 1 μm thick membrane.

We focused this work in determining the intrinsic (mixed matrix) material properties for gas separation. In future we will transfer membrane preparation into applied hollow fiber configuration. Hollow fibers are highly productive because have thin selective layer and can be densely packed into membrane modules with high membrane area. Bare 6FDA-DAM polymer was already shown to be spinnable into a hollow fiber structure [68]. Merkel *et al.* assessed the competitiveness of membrane separation technology for post-combustion CO_2 capture application [69]. They identified an optimum region of membrane properties (in terms of selectivity and permeance): the minimum CO_2/N_2 selectivity and CO_2 permeance required are 20 and 800 GPU (gas permeation unit), respectively. Lively et al. [22] have assessed the potential of 6FDA-based hollow fiber membranes for post-combustion CO_2 capture for the same process configuration proposed by Merkel *et al.* They concluded that if hollow fibers can be produced with a CO_2 permeance higher than 1000 GPU and CO_2/N_2 selectivity of 20, CO_2 capture cost could be reduced to less than 23 $/ton of CO_2. Extrapolating MMM results of our work, at an estimated selective layer thickness of 500 nm, gives mixed matrix hollow fiber with CO_2 permeability of 4620 GPU and CO_2/N_2 selectivity of 22. This is within the region of optimum membrane properties identified by Merkel *et al.* [61] for the separation of CO_2 from flue gas. Moreover, not only the 40 wt% ZIF-94 loaded membrane, but all the MMMs prepared in this work would be within this optimum region if they are transferred to a hollow fiber configuration (1850, 2280 and 2450 GPU of CO_2 for 10, 20 and 30 wt% ZIF-94 loaded MM HF respectively). Furthermore, the increase in CO_2 permeance at higher ZIF-94 loading would lead to significant reduction in total membrane area required, and hence in the reduction of investment cost for CO_2 capture, as reported by Lively *et al.* [22].

4. Conclusions

MMMs of ZIF-94 and glassy polyimide 6FDA-DAM have been successfully prepared up to high loadings of 40 wt%, using filler produced in up scaled and environmentally more benign process. Membranes are homogeneous and defect free with unaltered filler crystalline structure. Addition of filler increases gas membrane permeability in accordance to Maxwell model. An additional increase is observed at 40 wt% loading, attributed to the disruption of the chain packing of the polymer and increase in the polymer free volume. Separation performance of 40 wt% ZIF-94 loaded membrane developed in this work shows the highest permeability at similar selectivity among 6FDA-DAM MMMs reported in literature. For the first time membranes were characterized by non-invasive infrared scattering type scanning near field optical microscopy, which provides nanoscale-resolved chemical information that complements standard analysis methods. In the future, s-SNOM could be applied for more detailed nanoscale studies, for example of inhomogeneities, and chemical interaction, particularly at the interfaces between individual membrane components [52].

The developed MMM have great potential to be spun into a hollow fiber membrane configuration since the bare polymer is spinnable and the ZIF-94 filler has a smaller size than the selective layer (< 500 nm). Therefore, the region of optimal membrane properties for the separation of CO_2 from flue gas identified by Merkel *et al.* [69] can be amply reached with any of the MMMs prepared in this work (10–40 wt% ZIF-94 loading).

Acknowledgements

The authors acknowledge the financial support of the European Research Council under the European Union's Seventh Framework Programme *(FP/2007–2013)*, under grant agreement no. 608490, M4CO2 project, and the Spanish Ministry of Economy and Competitiveness (national project MAT2015-65525-R). The authors are very grateful to Gorka Imbuluzqueta (Tecnalia Research and Innovation, Spain) for the IR characterization of the samples. J.G. gratefully acknowledges support from the European Union Seventh Framework Programme *(FP7/2007–2013)*, ERC Stg, Grant Agreement n. 335746, CrystEng-MOF-MMM.

Appendix A. Supporting information

Supplementary data associated with this article can be found in the online version at http://dx.doi.org/10.1016/j.memsci.2017.12.033.

References

[1] CO_2 emissions from fuel combustion. Highlights (2016 edition), 2016.
[2] 2011 Technology Map of the European Strategic Energy Technology Plan (SET-Plan), 2011.
[3] Technology Roadmap. Carbon Capture and Storage.
[4] J.D. Figueroa, T. Fout, S. Plasynski, H. McIlvried, R.D. Srivastava, Advances in CO_2 capture technology—The U.S. Department of Energy's Carbon Sequestration Program, Int. J. Greenh. Gas. Control. 2 (2008) 9–20, http://dx.doi.org/10.1016/S1750-5836(07)00094-1.
[5] P. Bernardo, E. Drioli, G. Golemme, Membrane Gas Separation: a Review/State of the Art, Ind. Eng. Chem. Res. 48 (2009) 4638–4663, http://dx.doi.org/10.1021/ie8019032.
[6] M.A. Aroon, A.F. Ismail, T. Matsuura, M.M. Montazer-Rahmati, Performance studies of mixed matrix membranes for gas separation: a review, Sep. Purif. Technol. 75 (2010) 229–242, http://dx.doi.org/10.1016/j.seppur.2010.08.023.
[7] L.M. Robeson, Correlation of separation factor versus permeability for polymeric membranes, J. Memb. Sci. 62 (1991) 165–185, http://dx.doi.org/10.1016/0376-7388(91)80060-J.
[8] L.M. Robeson, The upper bound revisited, J. Memb. Sci. 320 (2008) 390–400, http://dx.doi.org/10.1016/j.memsci.2008.04.030.
[9] S. Smart, C.X.C. Lin, L. Ding, K. Thambimuthu, J.C. Diniz da Costa, Ceramic membranes for gas processing in coal gasification, Energy Environ. Sci. 3 (2010) 268–278, http://dx.doi.org/10.1039/B924327E.
[10] A. Ismail, L. David, A review on the latest development of carbon membranes for gas separation, J. Memb. Sci. 193 (2001) 1–18, http://dx.doi.org/10.1016/S0376-7388(01)00510-5.
[11] N. Kosinov, J. Gascon, F. Kapteijn, E.J.M. Hensen, Recent developments in zeolite membranes for gas separation, J. Memb. Sci. 499 (2016) 65–79, http://dx.doi.org/10.1016/j.memsci.2015.10.049.
[12] S. Basu, A.L. Khan, A. Cano-Odena, C. Liu, I.F.J. Vankelecom, Membrane-based technologies for biogas separations, Chem. Soc. Rev. 39 (2010) 750–768, http://dx.doi.org/10.1039/b817050a.
[13] J. Gascon, F. Kapteijn, B. Zornoza, V. Sebastián, C. Casado, J. Coronas, Practical approach to zeolitic membranes and coatings: state of the art, opportunities, barriers, and future perspectives, Chem. Mater. 24 (2012) 2829–2844, http://dx.doi.org/10.1021/cm301435j.
[14] E. Fernandez, K. Coenen, A. Helmi, J. Melendez, J. Zuñiga, D.A. Pacheco Tanaka, M. van Sint Annaland, F. Gallucci, Preparation and characterization of thin-film Pd–Ag supported membranes for high-temperature applications, Int. J. Hydrog. Energy 40 (2015) 13463–13478, http://dx.doi.org/10.1016/j.ijhydene.2015.08.050.
[15] J. Coronas, Present and future synthesis challenges for zeolites, Chem. Eng. J. 156 (2010) 236–242, http://dx.doi.org/10.1016/j.cej.2009.11.006.
[16] H. Vinh-Thang, S. Kaliaguine, Predictive models for mixed-matrix membrane performance: a review, Chem. Rev. 113 (2013) 4980–5028, http://dx.doi.org/10.1021/cr3003888.
[17] P.S. Goh, A.F. Ismail, S.M. Sanip, B.C. Ng, M. Aziz, Recent advances of inorganic fillers in mixed matrix membrane for gas separation, Sep. Purif. Technol. 81 (2011) 243–264, http://dx.doi.org/10.1016/j.seppur.2011.07.042.
[18] T. Rodenas, M. van Dalen, E. García-Pérez, P. Serra-Crespo, B. Zornoza, F. Kapteijn, J. Gascon, Visualizing MOF mixed matrix membranes at the nanoscale: towards structure-performance relationships in CO_2/CH4 separation over NH2-MIL-53(Al)@PI, Adv. Funct. Mater. 24 (2014) 268, http://dx.doi.org/10.1002/adfm.201470014.
[19] H. Yehia, T.J. Pisklak, J.P. Ferraris, K.J. Balkus, I.H. Musselman, Methane facilitated transport using copper(II) biphenyl Dicarboxylate-triethylenediamine/poly (3-Acetoxyethylthiophene) mixed matrix membranes, Polym. Prepr. Am. Chem. Soc. 45 (2004) 35–36.
[20] M. Rezakazemi, A. Ebadi, State-of-the-art membrane based CO_2 separation using mixed matrix membranes (MMMs): an overview on current status and future directions, Prog. Polym. Sci. 39 (2014) 817–861, http://dx.doi.org/10.1016/j.progpolymsci.2014.01.003.
[21] B. Seoane, J. Coronas, I. Gascon, M.E. Benavides, O. Karvan, J. Caro, F. Kapteijn, J. Gascon, Metal–organic framework based mixed matrix membranes: a solution for highly efficient CO_2 capture? Chem. Soc. Rev. 44 (2015) 2421–2454, http://dx.doi.org/10.1039/C4CS00437J.
[22] R.P. Lively, M.E. Dose, L. Xu, J.T. Vaughn, J.R. Johnson, J.A. Thompson, K. Zhang, M.E. Lydon, J.-S. Lee, L. Liu, Z. Hu, O. Karvan, M.J. Realff, W.J. Koros, A high-flux polyimide hollow fiber membrane to minimize footprint and energy penalty for CO_2 recovery from flue gas, J. Memb. Sci. 423–424 (2012) 302–313, http://dx.doi.org/10.1016/j.memsci.2012.08.026.
[23] V. Nafisi, M.-B. Hägg, Gas separation properties of ZIF-8/6FDA-durene diamine mixed matrix membrane, Sep. Purif. Technol. 128 (2014) 31–38, http://dx.doi.org/10.1016/j.seppur.2014.03.006.
[24] S.N. Wijenayake, N.P. Panapitiya, S.H. Versteeg, C.N. Nguyen, S. Goel, K.J. Balkus, I.H. Musselman, J.P. Ferraris, Surface Cross-Linking of ZIF-8/Polyimide Mixed Matrix Membranes (MMMs) for Gas Separation, Ind. Eng. Chem. Res. 52 (2013) 6991–7001, http://dx.doi.org/10.1021/ie400149e.
[25] S. Japip, H. Wang, Y. Xiao, T. Shung Chung, Highly permeable zeolitic imidazolate framework (ZIF)−71 nano-particles enhanced polyimide membranes for gas separation, J. Memb. Sci. 467 (2014) 162–174, http://dx.doi.org/10.1016/j.memsci.2014.05.025.
[26] V. Nafisi, M.-B. Hägg, Development of dual layer of ZIF-8/PEBAX-2533 mixed matrix membrane for CO_2 capture, J. Memb. Sci. 459 (2014) 244–255, http://dx.doi.org/10.1016/j.memsci.2014.02.002.
[27] T. Li, Y. Pan, K.-V. Peinemann, Z. Lai, Carbon dioxide selective mixed matrix composite membrane containing ZIF-7 nano-fillers, J. Memb. Sci. 425–426 (2013) 235–242, http://dx.doi.org/10.1016/j.memsci.2012.09.006.
[28] C. Cao, The study of 6FDA-polyimide gas separation membranes, National University of Singapore, 2003.
[29] M.R. Coleman, R. Kohn, W.J. Koros, Gas-separation applications of miscible blends of isomeric polyimides, J. Appl. Polym. Sci. 50 (1993) 1059–1064, http://dx.doi.org/10.1002/app.1993.070500614.
[30] M.R. Coleman, W.J. Koros, The transport properties of polyimide isomers containing hexafluoroisopropylidene in the diamine residue, J. Polym. Sci. Part B Polym. Phys. 32 (1994) 1915–1926, http://dx.doi.org/10.1002/polb.1994.090321109.
[31] L.M. Costello, W.J. Koros, Thermally stable polyimide isomers for membrane-based gas separations at elevated temperatures, J. Polym. Sci. Part B Polym. Phys. 33 (1995) 135–146, http://dx.doi.org/10.1002/polb.1995.090330114.
[32] H. Kawakami, M. Mikawa, S. Nagaoka, Formation of surface skin layer of asymmetric polyimide membranes and their gas transport properties, J. Memb. Sci. 137 (1997) 241–250, http://dx.doi.org/10.1016/S0376-7388(97)00198-1.
[33] D.W. Wallace, C. Staudt-Bickel, W.J. Koros, Efficient development of effective hollow fiber membranes for gas separations from novel polymers, J. Memb. Sci. 278 (2006) 92–104, http://dx.doi.org/10.1016/j.memsci.2005.11.001.
[34] A. Sabetghadam, B. Seoane, D. Keskin, N. Duim, T. Rodenas, S. Shahid, S. Sorribas, C. Le Guillouzer, G. Clet, C. Tellez, M. Daturi, J. Coronas, F. Kapteijn, J. Gascon, Metal organic framework crystals in mixed-matrix membranes: impact of the filler morphology on the gas separation performance, Adv. Funct. Mater. 26 (2016) 3154–3163, http://dx.doi.org/10.1002/adfm.201505352.
[35] M.S. Boroglu, A.B. Yumru, Gas separation performance of 6FDA-DAM-ZIF-11 mixed-matrix membranes for H2/CH4 and CO_2/CH4 separation, Sep. Purif. Technol. 173 (2017) 269–279, http://dx.doi.org/10.1016/j.seppur.2016.09.037.
[36] T.-H. Bae, J.R. Long, CO_2/N2 separations with mixed-matrix membranes containing Mg2(dobdc) nanocrystals, Energy Environ. Sci. 6 (2013) 3565–3569, http://dx.doi.org/10.1039/C3EE42394H.
[37] T.-H. Bae, J.S. Lee, W. Qiu, W.J. Koros, C.W. Jones, S. Nair, A high-performance gas-separation membrane containing Submicrometer-Sized Metal–Organic Framework, Cryst., Angew. Chem. Int. Ed. 49 (2010) 9863–9866, http://dx.doi.org/10.1002/anie.201006141.
[38] C. Zhang, Y. Dai, J.R. Johnson, O. Karvan, W.J. Koros, High performance ZIF-8/6FDA-DAM mixed matrix membrane for propylene/propane separations, J. Memb. Sci. 389 (2012) 34–42, http://dx.doi.org/10.1016/j.memsci.2011.10.003.
[39] W. Morris, N. He, K.G. Ray, P. Klonowski, H. Furukawa, I.N. Daniels, Y. a. Houndonougbo, M. Asta, O.M. Yaghi, B.B. Laird, A combined experimental-computational study on the effect of topology on carbon dioxide adsorption in zeolitic imidazolate frameworks, J. Phys. Chem. C. 116 (2012) 24084–24090, http://dx.doi.org/10.1021/jp307170a.
[40] A.M. Marti, D. Tran, K.J. Balkus, Fabrication of a substituted imidazolate material 1 (SIM-1) membrane using post synthetic modification (PSM) for pervaporation of water/ethanol mixtures, J. Porous Mater. 22 (2015) 1275–1284, http://dx.doi.org/10.1007/s10934-015-0005-y.
[41] S. Aguado, C.-H. Nicolas, V. Moizan-Basle, C. Nieto, H. Amrouche, N. Bats, N. Audebrand, D. Farrusseng, Facile synthesis of an ultramicroporous MOF tubular membrane with selectivity towards CO_2, New J. Chem. 35 (2011) 41–44, http://dx.doi.org/10.1039/C0NJ00667J.
[42] F. Cacho-Bailo, M. Etxeberria-Benavides, O. Karvan, C. Tellez, J. Coronas, Sequential amine functionalization inducing structural transition in an aldehyde-containing zeolitic imidazolate framework: application to gas separation membranes, CrystEngComm 19 (2017) 1545–1554, http://dx.doi.org/10.1039/C7CE00086C.
[43] R.W. Cheary, A. Coelho, A fundamental parameters approach to X-ray line-profile fitting, J. Appl. Crystallogr. 25 (1992) 109–121, http://dx.doi.org/10.1107/S0021889891010804.
[44] F. Keilmann, R. Hillenbrand, Near-field microscopy by elastic light scattering from a tip, Philos. Trans. R. Soc. Lond. Ser. A Math. Phys. Eng. Sci. 362 (2004) 787–805 ⟨http://rsta.royalsocietypublishing.org/content/362/1817/787.abstract⟩.

[45] N. Ocelic, A. Huber, R. Hillenbrand, Pseudoheterodyne detection for background-free near-field spectroscopy, Appl. Phys. Lett. 89 (2006) 101124.
[46] T. Taubner, R. Hillenbrand, F. Keilmann, Nanoscale polymer recognition by spectral signature in scattering infrared near-field microscopy, Appl. Phys. Lett. 85 (2004) 5064–5066, http://dx.doi.org/10.1063/1.1827334.
[47] F. Huth, A. Govyadinov, S. Amarie, W. Nuansing, F. Keilmann, R. Hillenbrand, Nano-FTIR absorption spectroscopy of molecular fingerprints at 20 nm spatial resolution, Nano Lett. 12 (2012) 3973–3978, http://dx.doi.org/10.1021/nl301159v.
[48] B. Zornoza, A. Martinez-Joaristi, P. Serra-Crespo, C. Tellez, J. Coronas, J. Gascon, F. Kapteijn, Functionalized flexible MOFs as fillers in mixed matrix membranes for highly selective separation of CO_2 from CH4 at elevated pressures, Chem. Commun. 47 (2011) 9522–9524, http://dx.doi.org/10.1039/C1CC13431K.
[49] S. Aguado, J. Canivet, D. Farrusseng, Facile shaping of an imidazolate-based MOF on ceramic beads for adsorption and catalytic applications, Chem. Commun. 46 (2010) 7999–8001, http://dx.doi.org/10.1039/C0CC02045A.
[50] J. Canivet, S. Aguado, C. Daniel, D. Farrusseng, Engineering the environment of a catalytic metal–organic framework by postsynthetic hydrophobization, ChemCatChem 3 (2011) 675–678, http://dx.doi.org/10.1002/cctc.201000386.
[51] R. Krutokhvostov, A.A. Govyadinov, J.M. Stiegler, F. Huth, A. Chuvilin, P.S. Carney, R. Hillenbrand, Enhanced resolution in subsurface near-field optical microscopy, Opt. Express 20 (2012) 593–600, http://dx.doi.org/10.1364/OE.20.000593.
[52] I. Amenabar, S. Poly, M. Goikoetxea, W. Nuansing, P. Lasch, R. Hillenbrand, Hyperspectral infrared nanoimaging of organic samples based on Fourier transform infrared nanospectroscopy, Nat. Commun. 8 (2017) 14402, http://dx.doi.org/10.1038/ncomms14402.
[53] O.C. David, D. Gorri, A. Urtiaga, I. Ortiz, Mixed gas separation study for the hydrogen recovery from H2/CO/N2/CO_2 post combustion mixtures using a Matrimid membrane, J. Memb. Sci. 378 (2011) 359–368, http://dx.doi.org/10.1016/j.memsci.2011.05.029.
[54] H. Lin, E. Van Wagner, R. Raharjo, B.D. Freeman, I. Roman, High-performance polymer membranes for natural-gas sweetening, Adv. Mater. 18 (2006) 39–44, http://dx.doi.org/10.1002/adma.200501409.
[55] S. Matteucci, Y. Yampolskii, B.D. Freeman, I. Pinnau, Transport of gases and vapors in glassy and rubbery polymers, Mater. Sci. Membr. Gas Vap. Sep, John Wiley & Sons, Ltd, 2006, pp. 1–47, http://dx.doi.org/10.1002/047002903X.ch1.
[56] J.E. Bachman, Z.P. Smith, T. Li, T. Xu, J.R. Long, Enhanced ethylene separation and plasticization resistance in polymer membranes incorporating metal – organic framework nanocrystals, 15, 2016. doi: http://dx.doi.org/10.1038/NMAT4621.
[57] T.C. Merkel, B.D. Freeman, R.J. Spontak, Z. He, I. Pinnau, P. Meakin, A.J. Hill, Sorption, transport, and structural evidence for enhanced free volume in Poly(4-methyl-2-pentyne)/Fumed silica nanocomposite membranes, Chem. Mater. 15 (2003) 109–123, http://dx.doi.org/10.1021/cm020672j.
[58] J. Ahn, W.-J. Chung, I. Pinnau, M.D. Guiver, Polysulfone/silica nanoparticle mixed-matrix membranes for gas separation, J. Memb. Sci. 314 (2008) 123–133, http://dx.doi.org/10.1016/j.memsci.2008.01.031.
[59] M. Josephine, C. Ordoñez, K.J.B Jr, J.P. Ferraris, I.H. Musselman, Molecular sieving realized with ZIF-8 / Matrimid ® mixed-matrix membranes, J. Memb. Sci. 361 (2010) 28–37, http://dx.doi.org/10.1016/j.memsci.2010.06.017.
[60] S. Qiu, M. Xue, G. Zhu, Metal-organic framework membranes: from synthesis to separation application, Chem. Soc. Rev. 43 (2014) 6116–6140, http://dx.doi.org/10.1039/C4CS00159A.
[61] C. Zhang, K. Zhang, L. Xu, Y. Labreche, B. Kraftschik, W.J. Koros, Highly scalable ZIF-based mixed-matrix hollow fiber membranes for advanced hydrocarbon separations, AIChE J. 60 (2014) 2625–2635, http://dx.doi.org/10.1002/aic.14496.
[62] B. Zornoza, T. Carlos, Mixed matrix membranes based on 6FDA polyimide with silica and zeolite microsphere dispersed phases, AIChE J. 61 (2015) 4481–4490, http://dx.doi.org/10.1002/aic.
[63] L. Ge, W. Zhou, V. Rudolph, Z. Zhu, Mixed matrix membranes incorporated with size-reduced Cu-BTC for improved gas separation, J. Mater. Chem. A 1 (2013) 6350–6358, http://dx.doi.org/10.1039/C3TA11131H.
[64] J. Hu, H. Cai, H. Ren, Y. Wei, Z. Xu, H. Liu, Y. Hu, Mixed-matrix membrane hollow fibers of Cu3(BTC)2 MOF and polyimide for gas separation and adsorption, Ind. Eng. Chem. Res. 49 (2010) 12605–12612, http://dx.doi.org/10.1021/ie1014958.
[65] A. Car, C. Stropnik, K.V. Peinemann, Hybrid membrane materials with different metal-organic frameworks (MOFs) for gas separation, Desalination 200 (2006) 424–426, http://dx.doi.org/10.1016/j.desal.2006.03.390.
[66] D. Fritsch, K.V. Peinemann, D. De Figueiredo Gomes, Composite material, in particular composite membrane, and process for the production of the same, US Pat., 7, 658,784, 2010.
[67] A.F. Bushell, M.P. Attfield, C.R. Mason, P.M. Budd, Y. Yampolskii, L. Starannikova, A. Rebrov, F. Bazzarelli, P. Bernardo, J. Carolus Jansen, M. Lanč, K. Friess, V. Shantarovich, V. Gustov, V. Isaeva, Gas permeation parameters of mixed matrix membranes based on the polymer of intrinsic microporosity PIM-1 and the zeolitic imidazolate framework ZIF-8, J. Memb. Sci. 427 (2013) 48–62, http://dx.doi.org/10.1016/j.memsci.2012.09.035.
[68] L. Xu, C. Zhang, M. Rungta, W. Qiu, J. Liu, W.J. Koros, Formation of defect-free 6FDA-DAM asymmetric hollow fiber membranes for gas separations, J. Memb. Sci. 459 (2014) 223–232, http://dx.doi.org/10.1016/j.memsci.2014.02.023.
[69] T.C. Merkel, H. Lin, X. Wei, R. Baker, Power plant post-combustion carbon dioxide capture: an opportunity for membranes, J. Memb. Sci. 359 (2010) 126–139, http://dx.doi.org/10.1016/j.memsci.2009.10.041.